

First experiment with decelerated bare uranium ions conducted at the ESR storage ring

Th. Stöhlker^a, H. Reich^b, K. Beckert^b, F. Bosch^b, A. Gallus^b, H. Eickhoff^b,
B. Franzke^b, T. Kandler^b, O. Klepper^b, C. Kozhuharov^b, G. Menzel^b,
P.H. Mokler^b, F. Nolden^b, H.T. Prinz^b, P. Spädtke^b, M. Steck^b, T. Winkler^b,
R.W. Dunford^c, P. Rymuza^d, T. Ludziejewski^d, Z. Stachura^e, P. Swiat^f and
A. Warczak^f

^a *Institut für Kernphysik, August-Euler-Straße 6, D-60486 Frankfurt, and GSI-Darmstadt,
Postfach 110552, D-64220 Darmstadt, Germany*

^b *GSI-Darmstadt, Postfach 110552, D-64220 Darmstadt, Germany*

^c *Argonne National Laboratory, Argonne, IL, USA*

^d *Institut of Nuclear Physics, Swierk, Poland*

^e *Institut of Nuclear Physics, Krakow, Poland*

^f *University of Krakow, Poland*

The deceleration capabilities of the ESR have been used for the first time in a dedicated ground state QED experiment conducted at the gasjet target of the ring. By decelerating bare uranium ions from 358 MeV/u down to energies of as low as 49 MeV/u, X-ray spectra have been obtained which provide an abundant yield of characteristic X-ray transitions. The experiment demonstrates that, by choosing the appropriate beam energy and gasjet target, almost all excited projectile states can be selectively populated. Moreover, the experiment provides the first data for beam lifetimes of stored decelerated high- Z ions. Such data are essential for the design of future experiments dealing with decelerated ion beams far below 50 MeV/u.

1. Introduction

One promising experimental approach for the investigation of the effects of quantum electro-dynamics (QED) in strong Coulomb fields is a precise determination of the ground state transition energies in one-electron high- Z ions, e.g. uranium. Such challenging investigations are in particular sensitive to the higher-order QED corrections which cannot be tested for low- Z ions [1,2]. For high- Z ions, the ESR storage ring provides unique experimental conditions. This has already been demonstrated by experiments with substantially improved precision [3,4]. However, up to now,

the achieved experimental precision is still limited by uncertainties in the velocity determination and by counting statistics.

Here, we give a preliminary report on a dedicated X-ray experiment which was conducted recently for bare uranium ions at the gas target area of the ESR storage ring [5]. In order to overcome the drawbacks associated with fast moving X-ray sources the experiment was carried out at various beam energies. In particular, the deceleration mode of the ESR storage ring was applied for the first time. It provided bare uranium ions at moderate energies as low as 49 MeV/u which strongly reduced the uncertainties associated with the Lorentz transformation to the projectile system. These low beam energies reveal a new kind of characteristic X-ray spectrum which is not only of importance for atomic structure studies but also gives new detailed insight into the physics of ion-atom collisions. Moreover, the experiment provided the first experimental data for the beam lifetimes of high- Z decelerated ions, data which are of general relevance for the success of future experiments dealing with high- Z decelerated ions.

In section 2 the experimental X-ray detection setup at the gasjet target of the ESR will be described, as well as the experimental method used for the deceleration of the ions within the ESR. In section 3 the dependence of the beam lifetime on the ion energy is discussed with respect to electron pickup from the gasjet target by the projectiles. Here, special emphasis is given to the population of the excited projectile states by the electron capture processes which essentially determine the projectile X-ray emission characteristics. Thereafter, in section 4, a comparison between the X-ray spectra recorded at low and at high beam energies will be presented, where the new kind of X-ray spectra obtained for decelerated ions will be emphasized. Finally, in section 5, a short summary and outlook will be given.

2. Experimental method

A sketch of the storage ring ESR and of the experimental setup used at the gas target is given in fig. 1. It shows the reaction area which is surrounded by four Ge(i) X-ray detectors mounted at observation angles of 48° , 90° , and 132° with respect to the ideal ion-optical beam axis. The two detectors at 48° were installed symmetrically on opposite sides of the reaction chamber. One of the two is a conventional solid state detector equipped with an X-ray collimator slit in order to confine the angular acceptance and reduce the Doppler broadening. The other detector consists of seven equidistant, parallel segments, each furnished with separate readout. They deliver seven independent X-ray spectra, and the resulting sum spectrum combines the advantage of a large total solid angle with a narrow Doppler broadening of one segment. At 90° a very similar strip detector was used whereas at the 132° observation angle a conventional X-ray detector was installed. The detector geometry itself was precisely determined by laser assisted trigonometry [3].

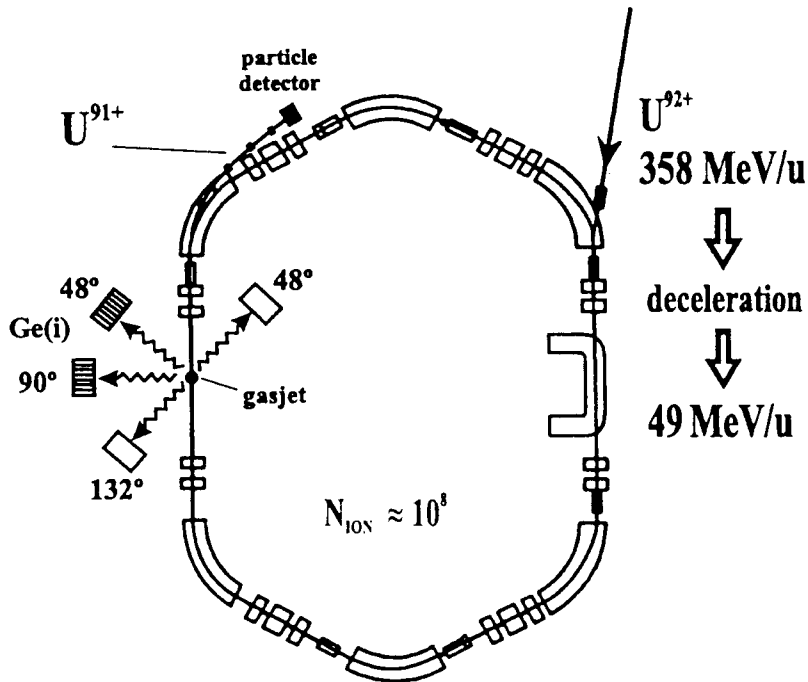


Fig. 1. Experimental arrangement at the ESR storage ring. The gasjet/beam interaction region is viewed by several Ge(i) X-ray detectors, two of them showing a high granularity. X-ray coincidences are measured with down-charged U^{91+} projectiles detected in the particle counter (PC) installed behind the next dipole magnet.

Bare uranium ions with an energy of 360 MeV/u delivered from SIS were injected into the ESR storage ring. Up to 10^{+8} stored ions were accumulated and cooled by utilizing an electron cooler current of 300 mA. The chosen cooler voltage determined the final energy of the circulating beam to be 358 MeV/u. At this energy the first part of the experiment was carried out using CH_4 , N_2 , and Ar reaction targets with thicknesses of about 10^{12} particles/cm². The X-ray emission produced via electron pickup from the gasjet particles into the fast moving ions was registered by the X-ray detector array in coincidence with the projectiles having captured one electron. For the latter purpose a fast plastic scintillator counter was used which was located behind the next dipole magnet in order to detect the down-charged ions from the gas target region (see fig. 1). In the second part of the experiment the deceleration option was applied. After finishing the stacking procedure which was still performed at the energy of 360 MeV/u, the coasting DC-beam was rebunched and decelerated while simultaneously ramping down the magnetic fields. Subsequently, electron cooling was switched on in order to balance the beam energy loss in the gas target and to fix the ion velocity to the chosen final beam energies of 220, 68, and 49 MeV/u. By applying this procedure up to 2×10^7 ions could be decelerated with a transmission efficiency of about 80%. At the two lowest beam energies, the electron cooler current was kept at a relatively low value of 50 mA in order to avoid a too strong reduction of the beam lifetime.

3. Cross sections and beam lifetimes

Experiments dealing with high- Z decelerated ions [6] require a precise estimation of beam losses caused by charge-exchange processes of the stored ions interacting with the residual gas atoms (molecules). In particular, in the case the ESR gasjet is needed, the large charge-exchange cross-sections at low energies may drastically reduce the lifetime of the stored ion beam. This may constitute the most serious limitation for such experiments, as the beam lifetime (τ) is connected to the charge-exchange cross-section (σ) by the relation

$$\lambda = 1/\tau = \rho \times \sigma \times f. \quad (1)$$

Here λ denotes the charge exchange rate, ρ the effective target thickness ($1/\text{cm}^2$) and f the revolution frequency of the circulating ion beam. It is important to note that in contrast to the high energy regime, up to now no experimental cross section data are available for bare or even few-electron high- Z ions colliding with atoms far below the production energy of the high projectile charge states.

In the following we consider only beam losses in the ring which are caused by charge exchange in the gasjet target. Beam losses due to charge exchange in the residual gas and due to radiative recombination in the electron cooler are also important subjects [7] which, however, can be neglected when using the gasjet target. For our beam lifetime studies with the decelerated bare uranium beams, a N_2 gasjet target with an areal density of $0.5 \times 10^{+12}$ particles/ cm^2 was applied and the beam lifetimes were determined from the charge-exchange rates measured by the particle detector for the down-charged U^{91+} ions. In fig. 2 the corresponding count rate spectra obtained at the various beam energies, normalized to one common scale, are given as a function of time. In addition, in table 1, the measured lifetimes are quoted. As shown in the figure the deceleration of the ion beam to energies as low as 49 MeV/u leads to a drastically reduced lifetime of about 1 min which has to be compared with the lifetime of about 20 min measured at 358 MeV/u. This is a consequence of the strongly enhanced electron pickup cross sections at low beam energies, where Non-Radiative Electron Capture (NRC) is by far the most important charge-exchange process [8], since its cross section scales as

$$\sigma_{\text{NRC}} \sim Z_{\text{T}}^5 \times Z_{\text{P}}^5 / v^{11}. \quad (2)$$

Here, v is the projectile velocity and Z_{P} and Z_{T} denote the nuclear charge of the projectile and of the target, respectively. The theoretical lifetimes given in table 1 were obtained by using the relativistic eikonal approximation for NRC [8] which is known to provide (within a factor of three) reliable cross section predictions for high and medium beam energies. In addition the calculation takes into account the competing Radiative Electron Capture (REC) process [9] by using the dipole approximation [10] which treats REC as the time reversed photoionization process. As seen in table 1, the theoretical lifetime data for the high energies are in good agreement with the experimental findings but seem to deviate markedly at the low energy of 49 MeV/u.

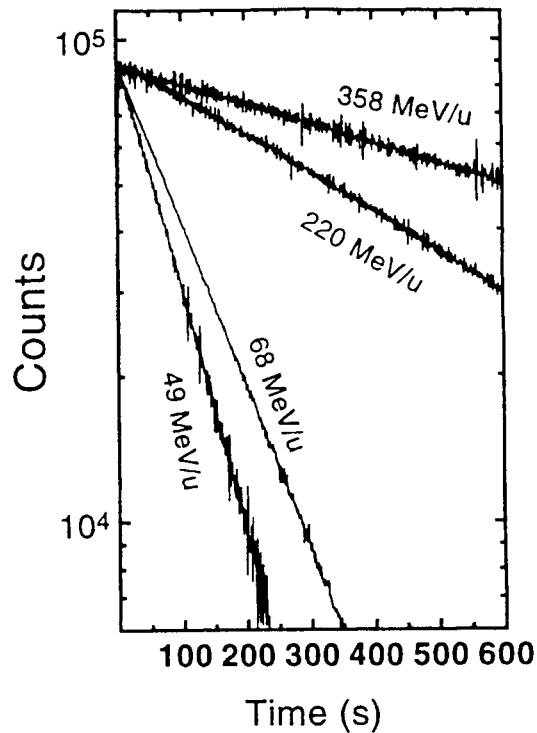


Fig. 2. Charge exchange rates of down-charged U^{91+} ions measured for various beam energies by the particle detector mounted downstream of the gasjet target behind the next dipole magnet (compare also fig. 1). The count rate spectra obtained at the various beam energies are normalized to one common scale. For the measurement at all four energies, a N_2 gasjet target with an areal density of $0.5 \times 10^{+12}$ particles/cm² was applied. The corresponding beam lifetimes are given in table 1.

Table 1

Experimental beam lifetimes measured for stored, bare uranium ions. For the measurement a N_2 gasjet target ($0.5 \times 10^{+12}$ particles/cm²) was used.

Beam energy (MeV/u)	Experimental (s)	Theory (s)
49	80	21
68	130	70
220	750	624
358	1300	1200

Here, one has to consider the imprecisely known overlap between the gasjet target and the ion beam. In order to obtain more reliable cross section data, the total charge exchange rates will be normalized to the measured K-REC X-ray intensities (see section 4) as the latter process has been studied in great detail by experiments and theory [9,11].

For completeness the theoretical cross section dependence on the beam energy and on the projectile main quantum number n_f are depicted in fig. 3 for NRC as well as for REC. These features are of particular relevance as the population of the excited

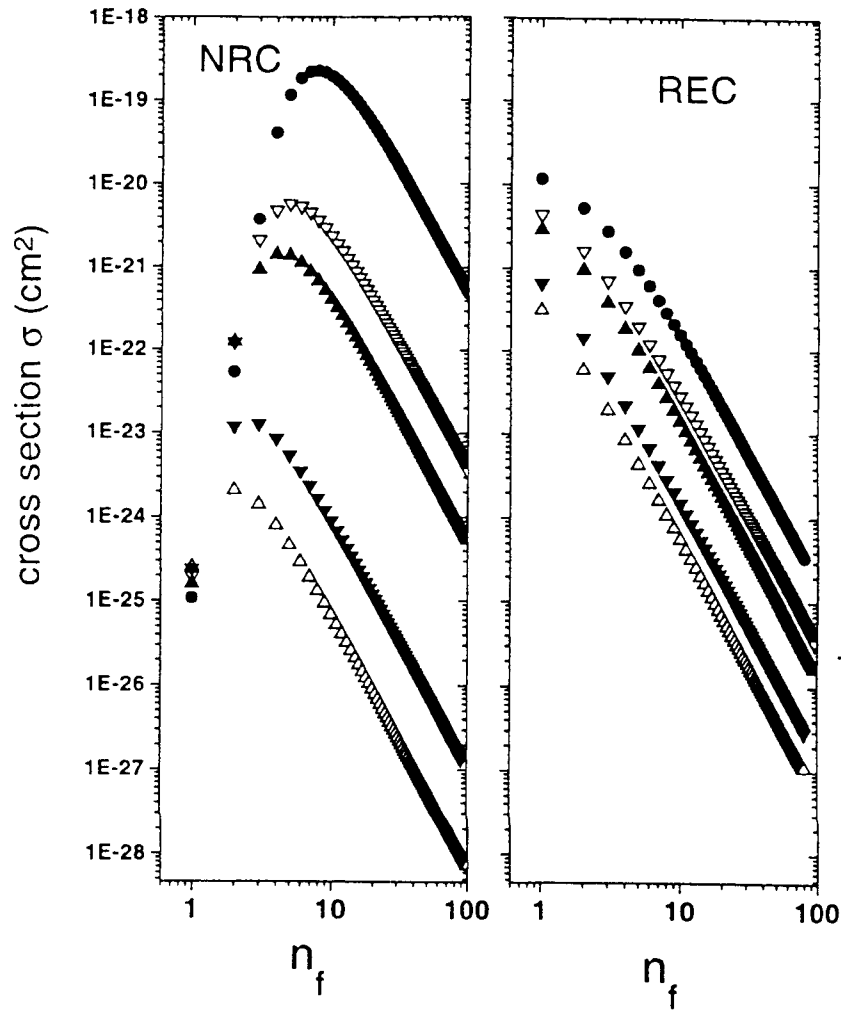


Fig. 3. Theoretical cross section dependencies on the projectile main quantum number for the two competing capture processes, REC [9] and NRC [8]. The cross sections are given for various beam energies (20 MeV/u: solid circles, 49 MeV/u: open down triangles, 68 MeV/u: solid up triangles, 220 MeV/u: solid down triangles; 358 MeV/u: open up triangles).

projectile states by electron capture from the target atoms (molecules) determine the projectile X-ray emission characteristics. Again, the calculations were performed for the collision system $U^{92+} \rightarrow N$ using the eikonal approximation for NRC and the dipole approximation for REC. As can be seen from fig. 3, REC is by far the dominant electron pickup process at high energies whereas NRC dominates in the low energy regime. Most importantly, NRC populates predominantly excited projectile levels whereas in the case of REC the population of the ground state is always the dominant capture channel.

4. X-ray transitions in hydrogen-like uranium

In the following we restrict the discussion of the first part of the experiment, carried out at the high energy of 358 MeV/u, to one typical coincident X-ray spectrum recorded

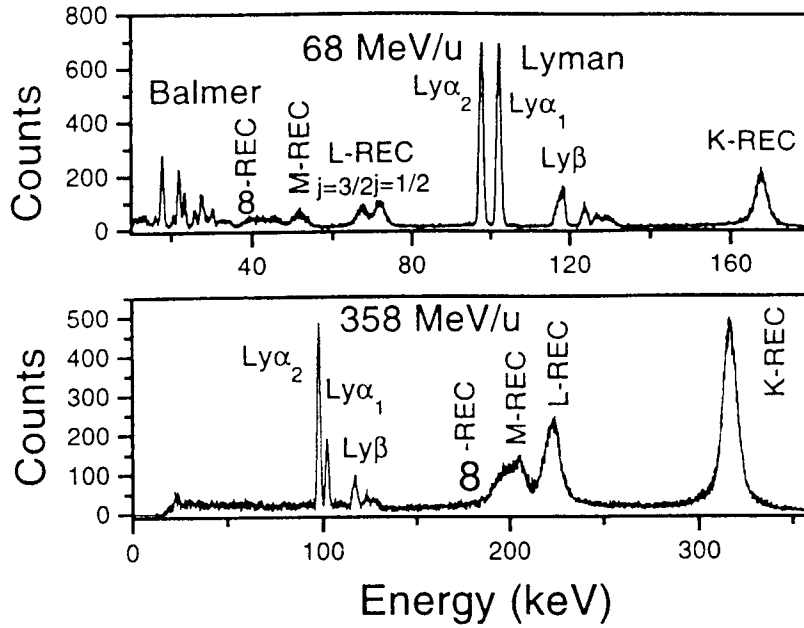


Fig. 4. X-ray spectrum (emitter system) of H-like uranium measured at 68 MeV/u (top) in comparison with the one recorded at 358 MeV/u (bottom).

at the backward angle of $\vartheta_{\text{lab}} = 132^\circ$ (compare fig. 4). Similar spectra have already been recorded in previous experiments and details about the corresponding spectrum analysis can be found in refs. [3,9]. In comparison to a former uranium experiment [3] a significant statistical improvement can be stated. Spectra with similar statistics have also been recorded for Ar and CH₄ reaction targets. Due to the high energy, corresponding to $\beta = 0.69$, Radiative Electron Capture (REC) is the only projectile charge-exchange process that has to be considered [9,11] (see fig. 3). Consequently, the spectrum is almost entirely dominated by REC transitions into the ground and excited states of the projectile. The latter lead via cascades to the well resolved characteristic Lyman- α transitions (i.e. Lyman- α_1 : $2p_{3/2} \rightarrow 1s_{1/2}$, Lyman- α_2 : $2p_{1/2} \rightarrow 1s_{1/2}$) which provide the most direct access to the ground state binding energy. Here, we have to add that the Lyman- α_2 line is blended by the $2s_{1/2} \rightarrow 1s_{1/2}$ M1 decay that is a prompt transition mode for uranium. However, due to the dominance of the K-REC process, only a small fraction of about 20% of the capture events produce such ground state transitions.

Compared to the high-energy regime, the X-ray spectra recorded for the decelerated ions provide an abundant yield of different characteristic projectile transitions. The upper spectrum in fig. 2 (observation angle 132°) was measured at the energy of 68 MeV/u in coincidence with electron capture. Again, the broader lines are caused by REC into the projectile. However, the relatively low collision velocity of $\beta = 0.36$ leads to a strong reduction of the Doppler broadening as well as of the width of the REC lines which is caused by the Compton profile of the target electrons [9]. As a result the REC transitions into the final j -sublevels of the L-shell appear well resolved. Note that the difference in the centroid energies between the K-REC and

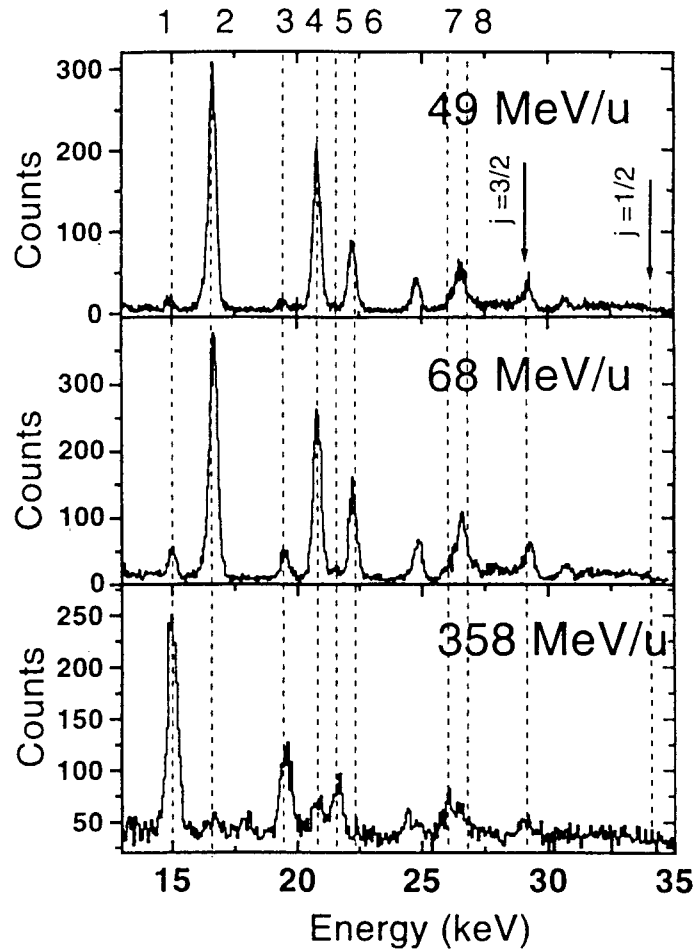


Fig. 5. Balmer spectra measured at 48° in coincidence with one-electron capture for bare uranium ions at 49 MeV/u (top), 68 MeV/u (middle), and 358 MeV/u (bottom). For line assignment compare the numbering at the very top of the figure with table 2.

the $j = 3/2$ L-REC lines should exactly correspond to the energy of the observed Lyman- α_1 ground state transition energy. It provides therefore a unique means for a redundant spectrum analysis. As discussed in the previous section, REC is no longer the dominant capture mechanism at low beam energies. Here, NRC into excited states contributes to a large extent to the total electron capture cross-section. Such capture events lead through cascades to Balmer ($n = 3, 4, \dots \rightarrow n = 2$) as well as to Lyman transitions ($n = 2, 3, 4, \dots \rightarrow n = 1$). The prominent Lyman lines in the spectrum demonstrate this behavior and the Balmer series is clearly identified in the spectrum. Obviously, the production of characteristic projectile X-rays is now much more efficient than at high energies where REC to the ground state prevails.

Complementary information to the Lyman spectrum is provided by the Balmer transitions. In fig. 5 the Balmer spectra (emitter system) are plotted as they were measured at the various beam energies by the conventional Ge(i) detector installed at 48° observation angle. In addition, the origin of the most prominent transition lines is explained in table 2 (compare numbers given in fig. 5 for the identification of the transition lines). Again, depending on the beam energy, the Balmer spectra show

Table 2

The most prominent Balmer transitions appearing in fig. 5. The numbers quoted in the first row refer to numbers given in the figure for line identification.

1	3s,p ($j = 1/2$) \rightarrow 2p	($j = 3/2$)
2	3d ($j = 5/2$) \rightarrow 2p	($j = 3/2$)
3	3s,p ($j = 1/2$) \rightarrow 2s, p	($j = 1/2$)
4	3p,d ($j = 3/2$) \rightarrow 2s, p	($j = 1/2$)
5	4s,p ($j = 1/2$) \rightarrow 2p	($j = 3/2$)
6	4d,f ($j = 5/2$) \rightarrow 2p	($j = 3/2$)
7	4s,p ($j = 1/2$) \rightarrow 2s, p	($j = 1/2$)
8	4p,d ($j = 3/2$) \rightarrow 2s, p	($j = 1/2$)

completely different intensity patterns. At 358 MeV/u the spectrum is dominated by $j = 1/2 \rightarrow j = 3/2$ dipole transitions. This can be explained by the population characteristics of REC which populates at high energies only low j -levels and, in particular, s-states. Moreover, as the dependence of the REC cross sections scales with $1/n^3$ [8], only a limited number of transitions show up in the spectrum. This is completely in contrast to the low beam energies. Here, a multitude of Balmer transitions are clearly distinguishable and transitions from high n states up to the series limit can be identified, which makes these spectra unique. Note the presence of two limits due to the $j = 1/2$ and $j = 3/2$ subshell splitting of the L-shell (marked by arrows in the spectra). These features not only verify the prediction that electron capture at low energies populates preferentially high n levels but they show in particular that NRC favors states with large angular momentum quantum numbers. Note that at the low beam energies transitions from $j = 1/2$ levels disappear almost completely.

5. Summary and outlook

The X-ray spectra measured for the decelerated uranium ions indicate a considerable progress for spectroscopy experiments dealing with high- Z ions. As discussed in detail in this paper, the abundant yield of different characteristic projectile transitions observed for the decelerated ions are a consequence of the population characteristics of excited projectile states by electron capture at low beam energies. It leads to very efficient Lyman α production, i.e. almost 70% of the electron capture events produce such X-ray transitions which are used for ground state QED investigations. Moreover, at low energies, the strongly enhanced electron pickup cross-sections in the gasjet target explain the short beam lifetimes measured. Most importantly, it was shown that by choosing the appropriate gas target and gas target density the stored ion beams can be used up efficiently, with a time constant of about one minute. Combined with the high intensity beams of about 10^8 bare uranium ions/s, already available from SIS,

and a strongly enhanced injection efficiency into the ESR, intense Lyman α radiation of about 5×10^5 photons per second and into 4π can be anticipated in the near future at the ESR. This will allow the implementation of high-resolution X-ray detection devices, such as crystal spectrometers [12] or bolometers [13], which are presently under construction. The latter instruments are urgently needed in order to push the absolute accuracy of the ground state QED experiments for high- Z systems towards ± 1 eV.

Moreover, the observed strong variation of the intensity patterns of the Balmer series with the beam energy are found to be well explained by the general cross-section scaling laws for the two relevant electron capture processes, i.e. REC and NRC. These spectra show that almost every excited level in high- Z H- and He-like ions can efficiently be populated by selecting the appropriate combination of beam energy and target- Z . This opens new possibilities to precision spectroscopy of high- Z ions. For example, the 2s-Lamb shift in heavy H-like ions and the QED corrections of the excited levels in He-like high- Z systems ($\Delta n = 0$ transitions) [14] now become accessible to experiment.

References

- [1] P.J. Mohr, Phys. Rev. A 46 (1993) 4421.
- [2] H. Persson, S. Salomonson, P. Sunnergren, I. Lindgren and M.G.H. Gustavsson, see contribution within this conference.
- [3] Th. Stöhlker, P.H. Mokler, K. Beckert, F. Bosch, H. Eickhoff, B. Franzke, M. Jung, Kandler, O. Klepper, C. Kozhuharov, R. Moshhammer, F. Nolden, H. Reich, P. Rymuza, P. Spädtke and M. Steck, Phys. Rev. Lett. 71 (1993) 2184.
- [4] H.F. Beyer, G. Menzel, D. Liesen, A. Gallus, F. Bosch, R. Deslattes, P. Indelicato, Th. Stöhlker, O. Klepper, R. Moshhammer, F. Nolden, H. Eickhoff, B. Franzke and M. Steck, Z. Phys. D 35 (1995) 169 and H.F. Beyer, IEEE Trans. Instr. Meas. 44 (1994) 510.
- [5] Th. Stöhlker, GSI-Nachrichten, 05–95, (1995) and P.H. Mokler, Th. Stöhlker, R.W. Dunford, A. Gallus, T. Kandler, G. Menzel, H.-Th. Prinz, P. Rymuza, Z. Stachura, P. Swiat and A. Warczak, Z. Phys. D 35 (1995) 274.
- [6] H. Poth et al., HITRAP, report GSI-90–20 (1990).
- [7] T. Winkler, K. Beckert, F. Bosch, H. Eickhoff, B. Franzke, O. Klepper, C. Kozhuharov, F. Nolden, H. Reich, P. Spädtke, M. Steck and Th. Stöhlker, GSI Scientific Report 1994, GSI 94–1 (1995).
- [8] J. Eichler and W. Meyerhof, *Relativistic Atomic Collisions* (Academic Press, San Diego, 1995).
- [9] Th. Stöhlker, C. Kozhuharov, P.H. Mokler, A. Warczak, F. Bosch, H. Geissel, R. Moshhammer and C. Scheidenberger, Phys. Rev. A 51 (1995) 2098.
- [10] M. Stobbe, Ann. Phys. 7 (1930) 661.
- [11] A. Ichihara, T. Shirai and J. Eichler, Phys. Rev. A 49 (1994) 1975.
- [12] H.F. Beyer, *Physics with Multiply Charged Ions*, ed. D. Liesen (Plenum Press, New York, 1995).
- [13] P. Egelhof, H.F. Beyer, D. McCammon, F. v. Feilitzsch, A. v. Kienlin, H.-J. Kluge, D. Liesen, J. Meier, S.H. Moseley and Th. Stöhlker, Nucl. Instr. Meth. in Phys. Res. A 370 (1996) 263.
- [14] Th. Stöhlker and A.E. Livingston, Acta Physica Polonica B 27 (1996) 441.